INTERNATIONAL ATOMIC ENERGY AGENCY
UNITED NATIONS EDUCATIONAL, SCIENTIFIC AND CULTURAL ORGANIZATION
INTERNATIONAL CENTRE FOR THEORETICAL PHYSICS
I.C.T.P., P.O. BOX 586, 34100 TRIESTE, ITALY, CABLE: CENTRATOM TRIESTE

SMR/697
6-Mag.Mult.

RESEARCH WORKSHOP ON CONDENSED MATTER PHYSICS
(21 June - 3 September 1993)

WORKING GROUP ON MAGNETIC MULTILAYERS
(9 - 13 August 1993)

ELECTRONIC PROPERTIES OF RANDOM MAGNETIC SURFACES

J. KUNDROVSKY
Institute of Physics
Czech. Academy Sci.
CZ-18040 Praha 8
CZECH REPUBLIC

Electronic properties of random magnetic surfaces

J. Kudrnovský

Institute of Physics, Czech Academy of Sciences,

CZ-180 40 Praha 8, Czech Republic

and

Institute of Technical Electrochemistry,

Technical University, A-1060 Wien, Austria

I. Turek

Institute of Physical Metallurgy, Czech Academy of Sciences,

CZ-616 62 Brno, Czech Republic

V. Drchal

Institute of Physics, Czech Academy of Sciences,

CZ-180 40 Praha 8, Czech Republic

P. Weinberger

Institute of Technical Electrochemistry,

Technical University, A-1060 Wien, Austria

We have developed a self-consistent spin-polarized Green's function technique within the local spin-density formalism which is suitable for an efficient and reliable description of the electronic and magnetic properties of random transition metal surfaces. The all-electron linear muffin-tin orbital method in the tight-binding representation is used to describe the electronic states, while the semi-infinite nature of the system is incorporated within the surface Green's function approach. The potentials are treated within the atomic sphere approximation including both the monopole and the dipole components of the charge density. The effect of disorder is treated within the coherent potential approximation. Applications to random FeCo overlayers on a non-random fcc Cu(001) substrate are shown.

1 Introduction

The study of low-dimensional magnetic systems such as surfaces, interfaces and overlayers, has attracted a great deal of attention in the last decade [1]. Such a study offers a number of promising practical applications in the area of magnetic recording and new device applications. The lowering of symmetry and of the coordination numbers as compared with the bulk, leads to a variety of interesting phenomena such as an enhanced magnetic moment at the surface, localized interface states, correlation between structure and magnetism, etc.

Several ab-initio numerical techniques based on the local spin density approximation (LSDA), including the full-potential linearized augmented plane wave (FLAPW) method [2], were developed to calculate the electronic and magnetic properties of materials with two-dimensional translational symmetry. Such electronic structure calculations played not only a key role in the understanding of a great amount of the experimental data but they were also able to predict new systems with desired technological properties. Such calculations rely mostly on the modelling of the semi-infinite geometry of the system either by a single slab [2, 3] or in terms of separated slabs within a supercell approach [4]. Despite of the success of this type of approach in providing an understanding of the electronic and magnetic properties of surfaces and interfaces, methods which do not suffer from the slab geometry became more and more important. In particular, the Green s function (GF) approach, which takes properly into account the symmetry at the surface, is very promising. Several surface Green's function techniques have been developed recently such as the layer Korringa-Kohn-Rostoker (LKKR) method [5], the embedded Green's function technique [6], and the surface Green's function (SGF) [7, 8] approach developed in the frame of the tight-binding linear muffin-tin orbital method (TB-LMTO) [9]. An extensive comparison of calculated work functions and surface energies using the full-potential LMTO method in a supercell geometry [4] and the LMTO-SGF technique [10] led to a very good agreement and proved the power and reliability of the LMTO-SGF approach for ab-initio surface electronic structure calculations. Very recently the LMTO-SFG approach was implemented also to the case of surfaces of magnetic crystals [11].

Recent progress in developing of sophisticated synthesis techniques, like the molecular beam epitaxy in ultrahigh vacuum, has led to the fabrication of ultrathin magnetic overlayers (down to one monolayer) deposited on a noble metal substrates, e.g. Fe or Co monolayers on a Cu(001) substrate. Such systems can serve as a model for the study of two-dimensional (2D) magnetism. The study of bulk magnetic properties of materials with varying environment like alloys of different compositions, enriched significantly the understanding of the nature of magnetism. Undoubtedly, the time has come for analogous studies of 2D itinerant ferromagnetism of binary alloys.

Methods based on slab or supercell geometries are of limited use for random surfaces because they require an excessive number of atoms to be represented as such. The Green's function approach based on multiple scattering approach, however, seems to be a suitable tool for the study of the combined effect of disorder and surface as demonstrated recently for random overlayers [12, 13], interfaces [14], and surfaces of random alloys [15, 16]. The only studied spin-polarized case is that of Ref. 14 for the case of a metallic interface with rather smooth changes of potentials at the transition region between two solids. No similar study exists for the case of random magnetic surfaces at the solid-vacuum interface.

In this paper we report on the implementation of a spin-polarized version of the LMTO-SGF method developed recently for non-magnetic random surfaces [12, 13, 15, 16] and its application to the case of a random magnetic overlayer on a noble metal substrate. As a case study we chose a disordered FeCo overlayer on an fcc Cu(001) substrate as a possible realistic model of 2D alloy magnetism. The choice of this system is supported by the facts of easy Fe-Co solubility and negligible Fe-Cu or Co-Cu solubilities together with the fact that pure Fe and Co monolayers were already successfully fabricated and studied theoretically. In addition, the corresponding three-dimensional counterparts, namely bulk bcc-based random FeCo alloys were extensively studied both experimentally and theoretically. For the $Fe_{100-x}Co_x/Cu(001)$ system we have calculated atom- and layer-resolved densities of states and corresponding magnetic moments as well as the work function through the whole concentration range.

2 Formalism

The main features of our method can be summarized as follows: (i) application of the all-electron tight-binding linear muffin-tin orbital (TB-LMTO) method [9] within the local spin density approximation (LSDA) to describe the electronic structure from first-principles; (ii) description of the semi-infinite geometry of the system using the surface Green's function (SGF) formalism within the principal layer (PL) concept [8]; (iii) use of the coherent potential approximation (CPA) approach extended to inhomogeneous systems like random overlayers, surfaces [12, 15] and interfaces; (iv) characterization of the vacuum region by empty spheres which represent the continuation of the semi-infinite solid to infinity on the vacuum side; (v) description of the potentials for the constituents within the atomic sphere approximation (ASA) [1], and (vi) inclusion of monopole and dipole terms of the charge density for the calculation of the Madelung potential [7] at the surface of the solid.

The starting point of our approach is the non-relativistic semi-infinite Hamiltonian in the orthogonal MTO representation [9]

$$H^{\sigma}_{RL,R'L'} = C^{\sigma}_{RL}\delta_{RR'}\,\delta_{LL'} + (\Delta^{\sigma}_{RL})^{1/2}\,\{S^0[1-\gamma^{\sigma}\,S^0]^{-1}\}_{RL,R'L'}\,(\Delta^{\sigma}_{R'L'})^{1/2}. \qquad (1)$$

In Eq. (1), R and R' are the site indices, L and L' refer to the orbital indices, and σ denotes the spin index ($\sigma = \uparrow, \downarrow$). The Hamiltonian is diagonal in σ only for collinear magnetic structures. The basis set consists of s-, p-, and d-orbitals ($L = (lm), l \leq 2$). The geometry of the problem enters the Hamiltonian only via the structure constant matrix S^0. Due to the semi-infinite nature of the problem, all layers parallel to the surface have in principle different local physical properties. In order to overcome this difficulty, we assume that from a certain layer on, the electronic properties of all subsequent layers are identical to those of the corresponding infinite system, namely either to a homogeneous substrate or to the vacuum. The system is thus considered to be divided into three regions: (i) a homogeneous semi-infinite bulk substrate, (ii) a homogeneous vacuum region represented by empty spheres and characterized by flat potentials, and (iii) an intermediate region consisting of several (M) layers where all inhomogeneities (chemical or electronic) are

located, and which consists of a few layers of empty spheres and a few top layers of the vacuum-solid interface. We neglect relaxations of surface layers as well as effects connected with different sizes of the overlayer atoms. Under these assumptions one can use the ideal bulk structure constant S^0.

The properties of individual atoms occupying the ideal lattice sites are characterized in general by random potential parameters X^σ_{RL} ($X = C, \Delta$, and γ). Note that due to self-consistency for charge and magnetization densities the potential parameters depend on the spin index σ and also on the site index R. The potential parameters have a simple physical meaning: they describe the energetic positions C^σ_{RL}, the widths Δ^σ_{RL}, and the distortions γ^σ_{RL} of the 'pure' $RL\sigma$-bands.

In order to perform the configurational averaging within the CPA [17] and to introduce two–dimensional translational symmetry [9], the orthogonal MTO representation is transformed to the so-called most-localized MTO representation. The corresponding Green's functions, $G^\sigma(z) = (z - H^\sigma)^{-1}$ and $g^\sigma(z) = (P^\sigma(z) - S)^{-1}$, are related by an exact scaling transformation [1, 9, 17]. The quantity S is the screened structure constant matrix with elements $S_{RL,R'L'}$, while $P^\sigma(z)$ is a site-diagonal potential function matrix with elements $P^\sigma_{RL}(z)$ which, in turn, are simple functions of the potential parameters $C^\sigma_{RL}, \Delta^\sigma_{RL}$, and γ^σ_{RL} . The potential functions are (i) randomly $P^{A,\sigma}_{RL}(z)$ and $P^{B,\sigma}_{RL}(z)$ at the surface of the random alloy, (ii) randomly $P^{A,\sigma}_{L}(z)$ and $P^{B,\sigma}_{L}(z)$ in the overlayer, and $P^{b,\sigma}_{RL}(z)$ in the non-random substrate. The potential functions $P^{v,\sigma}_{RL}(z)$ for the empty spheres are non-random and spin-dependent in the intermediate region, but spin-independent in the vacuum region.

The use of screened structure constants has two important advantages: (i) The configurational averaging within the CPA can be performed without additional constraints [17], since S is non-random by definition and $P^\sigma(z)$ is a random, but site-diagonal operator. (ii) The short-range character of S allows to introduce the concept [8] of principal layers, which greatly facilitates the theoretical treatment of the semi-infinite geometry of the problem.

The configurationally averaged resolvent

$$\bar{g}(z) = \langle (P^\sigma(z) - S)^{-1} \rangle = (\mathcal{P}^\sigma(z) - S)^{-1} \tag{2}$$

is of central importance for the present formalism. In Eq.(2), $\mathcal{P}^\sigma(z)$ is the coherent potential function which describes the averaged motion of an electron in a random solid. $\mathcal{P}^\sigma(z)$ is found by solving the CPA equations for each layer in question [12, 15]

$$\begin{aligned} \sum_{\alpha=A,B} c^\alpha_p t^{\alpha,\sigma}_p(z) &= 0\,, \\ t^{\alpha,\sigma}_p(z) &= [P^{\alpha,\sigma}_p(z) - \mathcal{P}^\sigma_p(z)]\{1 + \Phi^\sigma_p(z)[P^{\alpha,\sigma}_p(z) - \mathcal{P}^\sigma_p(z)]\}^{-1}. \end{aligned} \tag{3}$$

Here, c^α_p are the layer-dependent concentrations of atoms $\alpha = A, B$ in a random binary alloy which are generally different from the bulk concentrations c^α_b in a few top layers (possible segregation of one of alloy components). For a particular site R_p in a given layer p, $t^{\alpha,\sigma}_p(z)$ and $\mathcal{P}^\sigma_p(z)$ are the on-site elements of the single-site t-matrix and of the coherent potential function, respectively. It should be noted that within the CPA the coherent potential function $\mathcal{P}^\sigma_p(z)$ is a site-diagonal operator [17]. The quantity $\Phi^\sigma_p(z) = \bar{g}^\sigma_{R_pR_p}(z)$ is the site–diagonal element of the configurationally averaged Green's function $\bar{g}^\sigma(z)$ for a given layer p, which depends on all related layer coherent potential functions $\mathcal{P}^\sigma_q(z)$. In other words, Eqs.(3) represent a set of coupled CPA equations for the layers in the intermediate region. In the case of a random overlayer, the CPA equations need to be solved only for the random overlayer. The evaluation of $\Phi^\sigma_p(z)$ will be discussed briefly below (see Eqs. 9 to 11). Finally, it should be noted that the quantities $t^{\alpha,\sigma}(z)$, $\mathcal{P}^\sigma(z)$, and $\Phi^\sigma_p(z)$ are matrices with respect to the orbital quantum numbers $L = (l, m)$. Due to the lowering of the symmetry at the surface, these matrices are non-diagonal with respect to L even for cubic lattices and $l \leq 2$. We recall that in the non-relativistic limit and for collinear magnetic structures, they are diagonal matrices in spin space. The coherent potential function matrix $\mathcal{P}^\sigma(z)$ for the system under consideration has the following form

$$\mathcal{P}^\sigma(z) = \begin{cases} P^\sigma(z) & \text{vacuum region} \\ \mathcal{P}^\sigma_p(z) & \text{layer p in the intermediate region} \\ \mathcal{P}^{b,\sigma}(z) & \text{bulk region.} \end{cases} \tag{4}$$

Note that the coherent potential function $\mathcal{P}_p^\sigma(z)$ is simply the potential function of the corresponding constituent for the layers without disorder, namely for the layers of empty spheres in the intermediate region and for the substrate layers in the overlayer case. The potential function $P^v(z)$ of the vacuum is known analytically [7] while for the ideal bulk $\mathcal{P}^{b,\sigma}(z)$ is determined from the charge self-consistent version of the bulk TB-LMTO-CPA method [17].

As already mentioned, the concept of the principal layers is a very useful theoretical tool for surface-related problems [8]. The semi-infinite solid can be partitioned into PLs such that only nearest-neighbor PLs are coupled by the structure constants. A principal layer can include one or more atomic layers depending on the orientation of the surface, the underlying crystal structure, and the screening of the structure constants S. It defines the characteristic dimension D of the problem, $D=n_{PL}(l_{max}+1)^2$, where n_{PL} is the number of atomic layers in a PL and l_{max} is the maximal angular momentum. The advantage of a tight-binding representation with fast decaying structure constants is thus obvious. In the following we shall limit ourselves to the simplest case, when the PL consists of one atomic layer with one atom per primitive cell. This includes a number of important low-index surfaces, e.g. the fcc(001) and fcc(111) faces (first nearest-neighbor terms in S), or the bcc(110) face (first and second nearest-neighbor terms in S).

Then, by employing translational symmetry parallel to the sample surface, one gets for the intralayer and interlayer structure constants

$$\begin{aligned} S_{pp}(k_\parallel) &= S_{00}(k_\parallel), \\ S_{pq}(k_\parallel) &= S_{01}(k_\parallel)\delta_{p+1,q} + S_{10}(k_\parallel)\delta_{p-1,q}, \end{aligned} \tag{5}$$

where

$$S_{pq}(k_\parallel) = \sum_{R\in\{R_{pq}\}} \exp\{ik_\parallel \cdot R_{pq}\} S(R_p - R_q). \tag{6}$$

Here, $k_\parallel$ is a vector from the surface Brillouin zone (SBZ), and R_{pq} denotes a vector which connects one site in layer p with other site in layer q. The bulk structure constants depend only on the difference vector $R_p - R_q$. It should be noted that the structure constants are independent of σ.

The configurationally averaged Green's function matrix

$$\bar{g}^\sigma(k_\parallel, z) = (\mathcal{P}^\sigma(z) - S(k_\parallel))^{-1} \tag{7}$$

is represented by an inverted infinite block-tridiagonal matrix with respect to the PL indices as it is seen from Eqs. (5) for the interlayer structure constants. A homogeneous semi-infinite system (bulk substrate or vacuum) for which the physical properties are identical in each layer, can be characterized by a single quantity, the surface Green's function (SGF) [8, 15]. By definition, the SGF is the top PL projection of the Green's function of the homogeneous semi-infinite bulk alloy or vacuum. The SGF can be determined directly in real space by using the technique developed in Ref. 8, which avoids the use of the bulk resolvent common to other approaches [7]. The SGFs for the bulk substrate $\mathcal{G}^{b,\sigma}(k_\parallel, z)$ and the vacuum $\mathcal{G}^{v,\sigma}(k_\parallel, z)$ are found from the equations

$$\begin{aligned} \mathcal{G}^{b,\sigma}(k_\parallel, z) &= (\mathcal{P}^{b,\sigma}(z) - S_{00}(k_\parallel) - S_{01}(k_\parallel)\,\mathcal{G}^{b,\sigma}(k_\parallel, z)\,S_{10}(k_\parallel))^{-1}, \\ \mathcal{G}^{v}(k_\parallel, z) &= (P^{\sigma}(z) - S_{00}(k_\parallel) - S_{10}(k_\parallel)\,\mathcal{G}^{v}(k_\parallel, z)\,S_{01}(k_\parallel))^{-1}, \end{aligned} \tag{8}$$

which have to be solved self-consistently for each $k_\parallel$ and energy $z = E + i\delta$. The equations for the SGFs (8) have a simple physical meaning: the first two terms on the r.h.s. of Eqs. (8) describe the inverse Green's function of an isolated layer of atoms, $[\mathcal{G}^{l,\sigma}(k_\parallel, z)]^{-1} = \mathcal{P}^\sigma(z) - S_{00}(k_\parallel)$, which is coupled to the semi-infinite bulk and vacuum system by the SGFs, $\mathcal{G}^{b,\sigma}(z)$ and $\mathcal{G}^{v,\sigma}(z)$, respectively. These SGFs provide the necessary coupling of the intermediate region to the semi-infinite bulk substrate and vacuum. For the (p, q) block $(1 \le p, q \le M)$ of the inverse configurationally averaged Green's function $\bar{g}^\sigma(k_\parallel, z)$ one gets

$$\{\bar{g}^\sigma(k_\parallel, z)\}^{-1}_{pq} = \{\mathcal{P}_p^\sigma(z) - S_{00}(k_\parallel) - \Gamma_p^\sigma(k_\parallel, z)\}\delta_{pq} - S_{01}(k_\parallel)\delta_{p+1,q} - S_{10}(k_\parallel)\delta_{p-1,q}, \tag{9}$$

where

$$\begin{aligned} \Gamma_1^\sigma(k_\parallel, z) &= S_{10}(k_\parallel)\mathcal{G}^v(k_\parallel, z)S_{01}(k_\parallel), \\ \Gamma_p^\sigma(k_\parallel, z) &= 0 \qquad \text{for } p = 2, 3, ..., M-1, \\ \Gamma_M^\sigma(k_\parallel, z) &= S_{01}(k_\parallel)\mathcal{G}^{b,\sigma}(k_\parallel, z)S_{10}(k_\parallel). \end{aligned} \tag{10}$$

Here $\mathcal{P}_p^\sigma(z)$ are the corresponding elements of the coherent potential function in the intermediate region (see Eq.(4)). The quantities Γ_1^σ and Γ_M^σ have the meaning of embedding potentials of the intermediate region to the vacuum and bulk regions, respectively. In other words, the concept of the SGF allows to reduce the original problem of an infinite order in PL indices to an effective problem of finite order M in PL indices.

The desired quantity $\Phi_p^\sigma(z)$ is then obtained by integrating the (p,p) block of $\bar{g}^\sigma(k_\parallel, z)$ over the SBZ:

$$\Phi_p^\sigma(z) = \bar{g}^\sigma_{R_p R_p}(z) = \frac{1}{N_\parallel} \sum_{k_\parallel} \bar{g}^\sigma_{pp}(k_\parallel, z). \tag{11}$$

In this equation, $N_\parallel$ is the number of atoms in a given layer p. The quantity $\Phi_p^\sigma(z)$, in turn, determines the layer-, component-, and spin-resolved charge density $\rho_p^{\alpha,\sigma}(r)$ relevant for the LSDA part of the problem:

$$\rho_p^{\alpha,\sigma}(r) = \sum_{L,L'} \int^{E_F} \Psi_{pL}^{\alpha,\sigma}(r,E)\, D_{p,LL'}^{\alpha,\sigma}(E)\, \Psi_{pL'}^{\alpha,\sigma}(r,E)\, dE. \tag{12}$$

Here, $\Psi_{pL}^{\alpha,\sigma}(r,E) = R_{pl}^{\alpha,\sigma}(|r|,E) Y_L(\hat{r})$ is a partial wave normalized to unity within the atomic sphere of radius s^α, $r = (|r|, \hat{r})$, and E_F is the substrate Fermi level. The quantity $D_{p,LL'}^{\alpha,\sigma}(E)$, which might be termed the local density of states matrix, is given by

$$D_{p,LL'}^{\alpha,\sigma}(E) = -\frac{1}{\pi} \mathrm{Im} F_{p,LL'}^{\alpha,\sigma}(E + i0), \tag{13}$$

$$F_{p,LL'}^{\alpha,\sigma}(z) = \left[\frac{P_{pL}^{\alpha,\sigma}(z)}{dz}\right]^{1/2} (\Phi_p^\sigma(z)\{1 + [P_p^{\alpha,\sigma}(z) - \mathcal{P}_p^\sigma(z)]\Phi_p^\sigma(z)\}^{-1})_{LL'} \left[\frac{P_{pL'}^{\alpha,\sigma}(z)}{dz}\right]^{1/2}.$$

Note that $F_p^{\alpha,\sigma}(z)$ is the on-site element of the conditionally averaged Green's function [15, 17] in the orthogonal MTO representation. The radial part $R_{pl}^{\alpha,\sigma}(|r|,E)$ of a partial wave is the regular solution of the radial Schrödinger equation corresponding to the following spin-polarized spherical LSDA potential

$$V_p^{\alpha,\sigma}(|r|) = -\frac{2Z^\alpha}{|r|} + V_{H,p}^\alpha(|r|; [\tilde{\rho}_p^\alpha]) + V_{xc,p}^{\alpha,\sigma}(\tilde{\rho}_p^\alpha(|r|), \tilde{m}_p^\alpha(|r|)) + V_p^{Mad}, \tag{14}$$

where

$$\begin{aligned} V_p^{Mad} &= \sum_L \sum_q M_{pq}^{sL} \bar{Q}_q^L, \\ \bar{Q}_p^L &= \sum_{\alpha=A,B} c_p^\alpha \left(\frac{\sqrt{4\pi}}{2l+1} \int_0^{s^\alpha} |r|^l Y_L(\hat{r})\, \rho_p^\alpha(r)\, d^3r - Z^\alpha \delta_{l,0} \right), \\ \rho_p^\alpha(r) &= \rho_p^{\alpha,\uparrow}(r) + \rho_p^{\alpha,\downarrow}(r), \quad m_p^\alpha(r) = \rho_p^{\alpha,\uparrow}(r) - \rho_p^{\alpha,\downarrow}(r). \end{aligned} \tag{15}$$

In Eqs. (14,15) Z^α is the atomic number of a given atom $\alpha = A, B$ in a random alloy. The first three terms in (14) are in turn the atomic Coulomb potential, the Hartree and the spin-polarized exchange-correlation term. Note that both spin-up and spin-down charge densities or, equivalently, the total charge $\tilde{\rho}_p^\alpha(|r|)$ and magnetization $\tilde{m}_p^\alpha(|r|)$ densities are needed in the exchange-correlation part of the potential. The superscript tilda indicates the spherically-symmetric part of the charge density. The last term in (14), the Madelung contribution, is the averaged electrostatic potential acting on electrons in the p-th layer. It originates from the redistribution of the electron density (as compared with the bulk one) in the various layers due to the presence of the surface and of the chemical heterogeneity. The generalized intralayer and interlayer Madelung constants M_{pq}^{sL} describe such interactions. The quantity $\bar{Q}_p^L$ is the configurationally averaged multipole moment of the non-spherical charge density in the p-th layer. We include not only the monopole $(l = 0, m = 0)$ but also the dipole $(l = 1, m = 0)$ contributions [10], whereby the axis of quantization is perpendicular to the surface. The Madelung potential is then obtained as a spherically averaged field generated by these monopoles and dipoles. Similarly, the electrostatic dipole barrier B_{di_p} across the surface has contributions both from the net charges ($\bar{q}_p = \bar{Q}_p^{l=0}$) and from the dipole moments ($\bar{d}_p = \sqrt{3}\, \bar{Q}_p^{l=1,m=0}$) in spheres. Details of the derivation of Madelung constants M_{pq}^{sL} are given in the Appendix to Ref. 16.

Finally, layer-resolved densities of states (DOS) and layer-resolved spectral densities $A_p(k_\parallel, E)$ can be determined by transforming back to the original orthogonal MTO representation. For example, the layer-DOS resolved with respect to component α, orbital quantum number L, and spin σ is given directly by the quantity $D_{p,LL}^{\alpha,\sigma}(E)$, Eq.(13), the on-site element of the physical Green's function. By integrating the spin-resolved layer DOSs up to the Fermi level E_F, the corresponding integral DOSs and local magnetic moments are found. The expression for $A_p(k_\parallel, E)$ is more involved as it requires also the knowledge of the conditionally averaged site off-diagonal elements of the physical Green's function. Its explicit form can be found in Ref. 17.

3 Numerical results and discussion

The theory developed in Sec. 2 is illustrated here for the case of random $Fe_{100-x}Co_x$ overlayers on an fcc(001) face of Cu. The CPA part of the problem is solved for the overlayer only, and separately for each spin orientation $\sigma = \uparrow$ (majority spin) and $\sigma = \downarrow$ (minority spin). The $k_\parallel$-space integration in Eq. (11) was performed over the irreducible part of the surface Brillouin zone of the fcc(001) surface using 21 special $k_\parallel$-points [18]. The LSDA part of the problem requires an evaluation of integrals over the energy interval (E_{min}, E_F). We substituted this integral by an integral over a semi-circle in the complex energy plane which starts at E_{min} below the occupied part of the spectra and ends at E_F, using typically 10 to 15 energy points and the Gaussian quadrature method. The intermediate layer consists of three sample layers (an overlayer and two top substrate layers) plus two layers of empty spheres at the vacuum-solid interface. In this region the potentials are varied until the self-consistency with respect to both CPA and LSDA is obtained. The Vosko-Wilk-Nusair form [19] of the exchange-correlation functional was used. The charge self-consistent bulk TB-LMTO calculations to determine $\mathcal{P}^b(z)$ and Fermi level were actually performed by coupling the ideal 'left' and 'right' semi-infinite crystals [13]. In this way, a maximum internal consistency for the bulk and surface calculations can be obtained as all involved Brillouin zone integrations are performed over the same, surface Brillouin zone.

The layer-resolved DOSs for a random paramagnetic $Fe_{50}Co_{50}$ overlayer on Cu(001) are shown in Fig. 1. The high value of the overlayer DOS at the Fermi level indicates the tendency of the system to form a magnetic phase thereby lowering its energy. The first substrate layer is significantly influenced by the overlayer as a result of the large d-level separation between Cu- and Fe- and/or Co-atoms. This is obvious after comparison with the corresponding DOSs of a clean Cu(001) crystal. The second substrate layer is influenced only weakly and is essentially bulk-like.

The layer- and component-resolved DOSs for a random ferromagnetic $Fe_{50}Co_{50}$ overlayer on Cu(001) are plotted in Figs. 2 and 3 for up- and down-spin, respectively. The spin splitting effectively decreases (increases) the separation of the Cu- and Fe- and/or

Co- d-levels. This reflects the stronger influence of the first substrate layer DOS by the overlayer in the down-spin case. The up- and down-spin electrons behave differently as well with respect to the alloy disorder. While the rigid-band-like behaviour of the up-spin electrons is obvious, the down-spin electrons experience a stronger disorder as can be seen from the different component Fe- and Co-DOSs. A similar effect was observed in random bcc bulk FeCo alloys [20].

The overlayer DOSs over the whole concentration range are plotted in Figs. 4 and 5 for up-spin and down-spin cases, respectively. We observe strong ferromagnetism stabilized by the substrate throughout the whole concentration range: the up-spin alloy bands are filled and hardly influenced by disorder in the overlayer. The corresponding down-spin alloy bands show a considerable narrowing with increasing Co-concentration. This is in contrast with the concentration independent alloy bandwidhts of bcc FeCo bulk alloys [20]. On the contrary, the corresponding level disorder as measured by a quantity $\delta = (C_{d\downarrow}^{Fe} - C_{d\downarrow}^{Co})/w^{alloy}$, where w^{alloy} is the averaged alloy bandwidth, is nearly twice as strong in the bulk case. These differences can be traced down to the basic difference between 3D alloy magnetism and 2D overlayer alloy magnetism. In the latter case the Fermi level is fixed by the substrate and charge neutrality in the system is achieved at the cost of the reconstruction of the electronic structure at the surface. In the bulk alloy the charge neutrality is achieved simply via a shift of the Fermi level to accommodate the corresponding number of electrons. This interesting phenomenon deserves, however, a more detailed consideration.

The magnetic properties of random overlayers are summarized in Table 1. The results for Fe and Co monolayers on fcc Cu(001) substrate, m_{ov}^{Fe} =2.80 μ_B and m_{ov}^{Co} =1.80 μ_B, compare reasonably well with the corresponding values obtained by a slab FLAPW method [21]: m_{ov}^{Fe} =2.69 μ_B and m_{ov}^{Co} =1.79 μ_B. The Fe-magnetic moment in Fe/Cu(001) is largely enhanced as compared to the bulk-like bcc Fe-moment (2.25 μ_B), while the Co-moment in Co/Cu(001) is only slightly higher than the bulk-like bcc Co-moment (1.70 μ_B). The bulk values were calculated consistently by a spin-polarized version of the TB-LMTO-CPA method. In accordance with FLAPW calculations [21] we note a very weak polarization of top substrate layers.

The calculated linear decrease of the averaged overlayer magnetic moment with the Co-concentration is a direct consequence of the stabilization of the strong ferromagnetism in terms of the substrate Fermi level. The local Fe- and Co-moments exhibit very weak concentration dependence as their up-spin bands are filled and there is no possibility to increase their occupation and thereby corresponding magnetic moments. This situation should be contrasted with the case of bulk bcc FeCo alloys, where the weak ferromagnetism of Fe gives the possibility to fill approximately 0.3 spin-up holes with spin-down electrons and thus to increase the local Fe moment by about 0.6 μ_B at the Co-rich end [20].

The calculated work functions of Fe/Cu(001) and Co/Cu(001) overlayers agree well with the corresponding FLAPW values (see Table 2). The slightly higher values obtained in present calculations are compatible with similar trends found for paramagnetic surfaces [10]. Note, however, the nearly perfect agreement for difference of the work functions of Fe/Cu(001) and Co/Cu(001) overlayers in both calculations. The calculated work functions of random FeCo/Cu(001) overlayers increase monotonically and almost linearly with the Co concentration, as to be expected from the higher value of the Co/Cu(001) work function as compared to the Fe/Cu(001) one.

4 Conclusions

We have given an account of an efficient self-consistent Green's function method to calculate electronic and magnetic properties of random surfaces of transition metals. The approach is based on the local spin density approximation within the all-electron first-principles tight-binding linear muffin-tin orbital method. The short-range character of intralayer and interlayer interactions facilitates the use of the surface Green's function approach which takes proper account of the reduced symmetry at the surface. The effect of disorder is included in the coherent potential approximation.

We have applied the formalism to the case of random FeCo overlayers on a fcc Cu(001) substrate. In the cases of the pure Fe and Co monolayers our results for magnetic moments and work functions are in very good agreement with recent full-potential slab calculations. The averaged magnetization of a random overlayer depends linearly on the composition

since the strong ferromagnetism is stabilized by the substrate over the whole composition range. As a consequence of the greater exchange splitting of Fe, the majority spin electrons behave rigid-band-like whereas a strong influence of alloy disorder in the overlayer on the minority spin electrons is found.

Electronic structure calculations like the present ones in the conjunction with the generalized perturbation method are the starting point for the use of an effective Ising model in the study of order-disorder transitions in the presence of magnetic moments. A more detailed study of disordered bcc FeCo alloys and of disordered FeCo overlayers on the Cu(001) substrate is necessary for a deeper understanding of the basic differences between itinerant alloy magnetism in three and two dimensions. Such an approach is beyond the scope of the present paper and will be subject of forthcoming publications.

Acknowledgements

Financial support of the Czech Academy of Sciences (Project No. 11015) and the Austrian Science Foundation (P8918) is acknowledged.

Table 1: Calculated averaged (m_{ov}^{av}) and component resolved (m_{ov}^{α}, α=Fe, Co) magnetic moments for random FeCo overlayers on an fcc Cu(001) substrate. The magnetic moments in the first (m_1^{Cu}) and second (m_2^{Cu}) substrate layers are also given. All values are in Bohr magnetons. The values in brackets denote the corresponding single impurity case.

	Fe-layer	$Fe_{75}Co_{25}$	$Fe_{50}Co_{50}$	$Fe_{25}Co_{75}$	Co-layer
m_{ov}^{av}	2.798	2.550	2.307	2.057	1.797
m_{ov}^{Fe}	2.798	2.817	2.844	2.871	(2.891)
m_{ov}^{Co}	(1.728)	1.749	1.770	1.786	1.797
m_1^{Cu}	0.015	0.014	0.014	0.012	0.009
m_2^{Cu}	−0.010	−0.009	−0.007	−0.007	−0.007

Table 2: Calculated work functions (eV) for random FeCo overlayers on an fcc Cu(001) substrate. For the monolayer coverages we compare our results with available full-potential FLAPW calculations of Ref. 21 using a slab geometry.

	Fe-layer	$Fe_{75}Co_{25}$	$Fe_{50}Co_{50}$	$Fe_{25}Co_{75}$	Co-layer
this work	5.29	5.37	5.42	5.48	5.55
slab FLAPW	5.09				5.34

Figure Captions

Fig. 1: Layer-resolved densities of states of a random paramagnetic $Fe_{50}Co_{50}$ overlayer on the Cu(001) substrate. The density of states of a clean Cu(001) surface (shown in dots) and the bulk density of states are also given. The overlayer and first two substrate layers are denoted by ov, s1, and s2, respectively. The vertical lines denote the position of the substrate Fermi level.

Fig. 2: Spin-up layer- and component-resolved densities of states of a random ferromagnetic $Fe_{50}Co_{50}$ overlayer on a Cu(001) substrate: Fe (full line) and Co (dashed line). The bulk density of states is also given. First two substrate layers are denoted by s1, and s2, respectively. The vertical lines denote the position of the substrate Fermi level.

Fig. 3: Spin-down layer- and component-resolved densities of states of a random ferromagnetic $Fe_{50}Co_{50}$ overlayer on a Cu(001) substrate: Fe (full line) and Co (dashed line). The bulk density of states is also given. First two substrate layers are denoted by s1, and s2, respectively. The vertical lines denote the position of the substrate Fermi level.

Fig. 4: Concentration dependence of the spin-up layer-resolved densities of states of a random ferromagnetic $Fe_{100-x}Co_x$ overlayer on a Cu(001) substrate. The vertical lines denote the position of the substrate Fermi level.

Fig. 5: Concentration dependence of the spin-down layer-resolved densities of states of a random ferromagnetic $Fe_{100-x}Co_x$ overlayer on a Cu(001) substrate. The vertical lines denote the position of the substrate Fermi level.

References

[1] L. M. Falicov, D. T. Pierce, S. D. Bader, R. Gronsky, K. B. Hathaway, H. J. Hopster, D. N. Lambeth, S. S. P. Parkin, G. Prinz, M. Salamon, I. K. Schuller, and R. H. Victora, J. Mater. Research 5 (1990) 1299.

[2] A. J. Freeman and Ru-qian Wu, J. Magn. Magn. Mater. 100 (1991) 497.

[3] O. Jepsen, J. Madsen, and O. K. Andersen, Phys. Rev. B26 (1982) 2790.

[4] M. Methfessel, D. Hennig, and M. Scheffler, Phys. Rev. B46 (1992) 4816.

[5] J. M. Mac Laren, S. Crampin, D. D. Vvedensky, and J. B. Pendry, Phys. Rev. B40 (1989) 12164.

[6] J. E. Inglesfield and G. A. Benesh, Phys. Rev. B37 (1988) 6682.

[7] H. L. Skriver and N. M. Rosengaard, Phys. Rev. B43 (1991) 9538.

[8] B. Wenzien, J. Kudrnovský, V. Drchal, and M. Šob, J. Phys.: Condens. Matter 1 (1989) 9893.

[9] O. K. Andersen and O. Jepsen, Phys. Rev. Lett. 53 (1984) 2571.

[10] H. L. Skriver and N. M. Rosengaard, Phys. Rev. B46 (1992) 7157.

[11] M. Aldén, S. Mirbt, H. L. Skriver, N. M. Rosengaard, and B. Johansson, Phys. Rev. B46 (1992) 6303.

[12] J. Kudrnovský, B. Wenzien, V. Drchal, and P. Weinberger, Phys. Rev. B44 (1991) 4068.

[13] J. Kudrnovský, I. Turek, V. Drchal, P. Weinberger, N. E. Christensen, and S. K. Bose, Phys. Rev. B46 (1992) 4222.

[14] S. Crampin, R. Monnier, T. Schulthess, G. H. Schadler, and D. D. Vvedensky, Phys. Rev. B45 (1992) 464.

[15] J. Kudrnovský, P. Weinberger, and V. Drchal, Phys. Rev. B44 (1991) 6410.

[16] J. Kudrnovský, I. Turek, V. Drchal, P. Weinberger, S. K. Bose and A. Pasturel, Phys. Rev. B47 (1993) (in press).

[17] J. Kudrnovský and V. Drchal, Phys. Rev. B41 (1990) 7515.

[18] S. L. Cunningham, Phys. Rev. B10 (1974) 4988.

[19] S. H. Vosko, L. Wilk, and M. Nusair, Can. J. Phys. 58 (1980) 1200.

[20] R. Richter and H. Eschrig, J. Phys. F18 (1988) 1813.

[21] Chun Li, A. J. Freeman, and C. L. Fu, J. Magn. Magn. Mater. 83 (1990) 51.

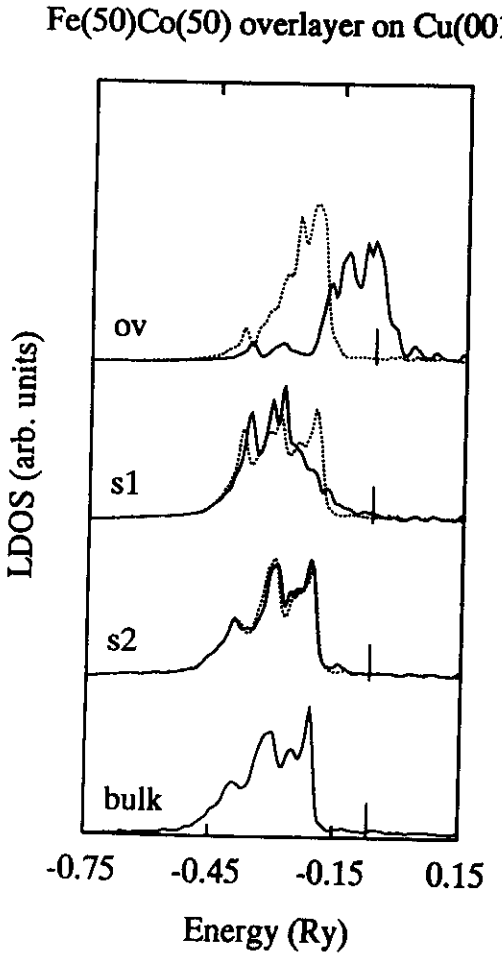
Fe(50)Co(50) overlayer on Cu(001)
LDOS (arb. units)
ov
s1
s2
bulk
-0.75
-0.45
-0.15
0.15
Energy (Ry)

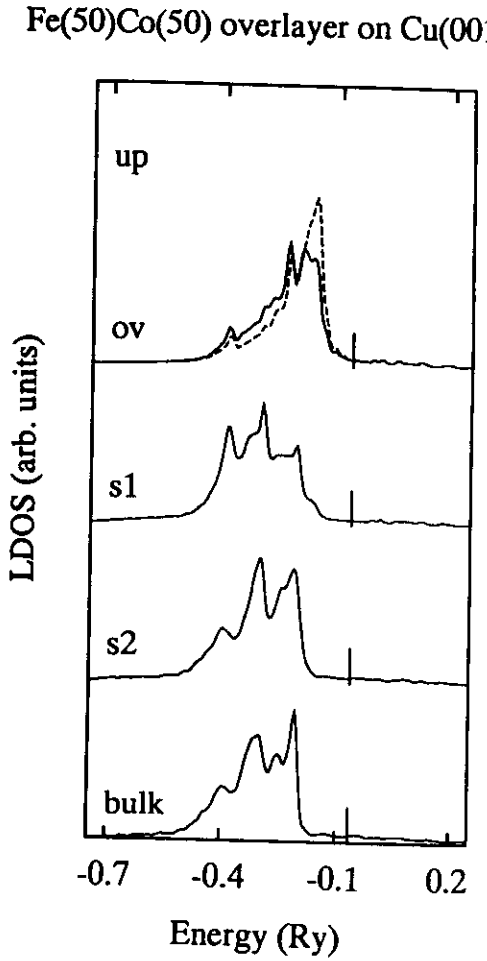
Fe(50)Co(50) overlayer on Cu(001)
LDOS (arb. units)
up
ov
s1
s2
bulk
-0.7
-0.4
-0.1
0.2
Energy (Ry)

Fig. 5

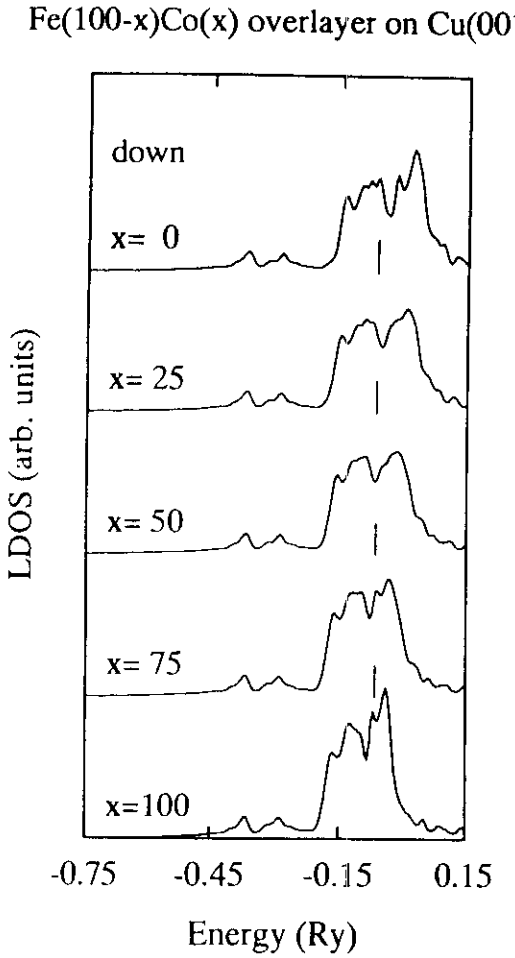
Fe(100-x)Co(x) overlayer on Cu(001)
down
x= 0
x= 25
x= 50
x= 75
x=100
LDOS (arb. units)
-0.75
-0.45
-0.15
0.15
Energy (Ry)

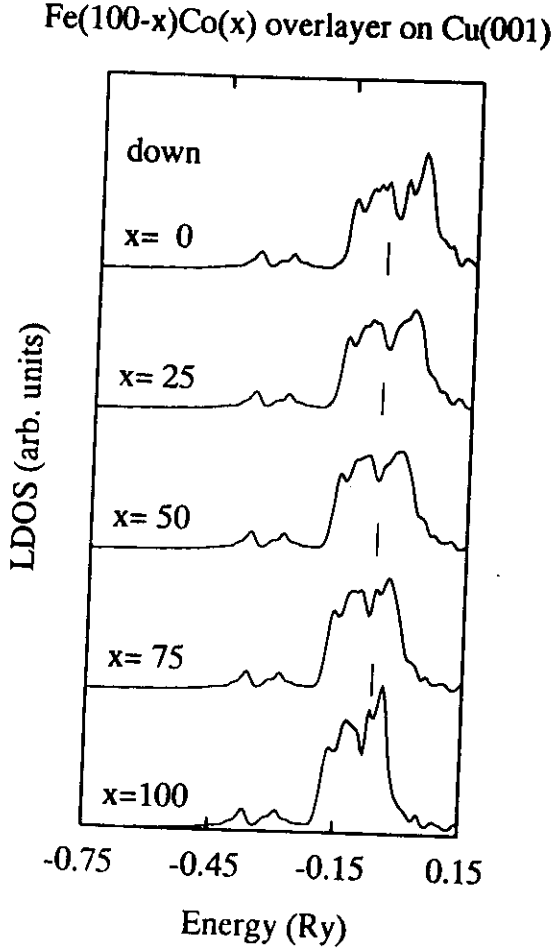
Fe(100-x)Co(x) overlayer on Cu(001)
down
x= 0
x= 25
x= 50
x= 75
x=100
LDOS (arb. units)
-0.75
-0.45
-0.15
0.15
Energy (Ry)